Growth evolution of ZnO films deposited by pulsed laser ablation

2001 J. Phys.: Condens. Matter 13 L663

(http://iopscience.iop.org/0953-8984/13/28/102)

INSTITUTE OF PHYSICS PUBLISHING JOURNAL OF PHYSICS: CONDENSED MATTER

J. Phys.: Condens. Matter **13** (2001) L663–L672 PII: S0953-8984(01)23501-2

LETTER TO THE EDITOR

Growth evolution of ZnO films deposited by pulsed laser ablation

E Vasco, C Zaldo and L Vázquez

Instituto de Ciencia de Materiales de Madrid, Consejo Superior de Investigaciones Científicas, Cantoblanco 28049 Madrid, Spain

E-mail: lvb@icmm.csic.es

Received 30 March 2001, in final form 4 June 2001
Published 29 June 2001
Online at stacks.iop.org/JPhysCM/13/L663

Abstract

We study the surface morphology evolution of ZnO films grown by pulsed laser deposition. Atomic force microscopy measurements show the existence of two growth regimes. Initially, the growth morphology is determined by shadowing effects due to the angular spreading of the plume in the 0.1 mbar oxygen working pressure. For longer deposition times a stepped pyramid-like structure is developed, whose roughening and coarsening behaviours are in agreement with those expected for growth systems with step-edge barriers.

1. Introduction

Many of the properties of thin films, which are the basis of their application in technological devices, depend on their surface properties, particularly on the surface roughness. Thus, the knowledge of the mechanisms that determine the film structure has motivated a large amount of research during the last years. In particular, a great effort has been given to the theoretical and experimental study of thin film growth evolution [1, 2]. Two characteristic lengths are usually employed to study the growth dynamics of different systems [3]: the width of the interface or surface roughness, σ (the rms height fluctuation around the mean height value) and a characteristic lateral correlation length, ξ, parallel to the surface. It is assumed that σ and ξ change with growth time, t, as $\sigma \sim t^{\beta}$ and $\xi \sim t^{p}$, respectively [3]. The exponents β and p depend on the growth mechanisms operating during deposition [1, 2], which determine the film morphology evolution. Thus, the experimental determination of these exponents and their comparison with the existing growth models allow us to identify the main growth mechanisms involved in the film deposition.

The focus of most of these film growth studies has been directed to single crystal surfaces or amorphous films rather than to polycrystalline ones, although the latter are the most employed coatings in many technological applications. However, although studies have been reported [4–6] on evaporated, sputtered and electrodeposited polycrystalline thin films, none have been reported, to our knowledge, on films prepared by pulsed laser deposition

(PLD). In fact, for PLD such theoretical approaches have been limited to the study of the initial nucleation stage [7]. This lack is surprising since PLD has become an outstanding technique in the preparation of thin films, especially oxides with different properties, namely superconductivity, magnetoresistance, ferroelectricity and electrooptics [8].

In this work, we study the growth dynamics of zinc oxide, ZnO, films grown by PLD. ZnO films are used in different applications, including SAW RF filters, chemical sensors and transparent electrodes of solar cells. ZnO films prepared by PLD show a very efficient exciton photoluminescence that is related to the very good crystalline quality achieved [9]. Under certain deposition conditions ZnO films display a hexagonal pyramidal surface morphology that can operate as nanosized Fabry–Perot resonators [10]. Thus, special interest has been paid in this work to the formation of these pyramidal structures.

2. Experimental details

ZnO samples were deposited on InP(100) substrates by PLD. A KrF excimer laser ($\lambda = 248$ nm, $I_{max} = 300$ mJ/pulse operated at 10 Hz) was focussed with an energy density of 4 J cm^{-2} on ZnO (99.99%) ceramic targets rotating at 20 rpm. The base pressure of the deposition chamber was 8×10^{-7} mbar and ZnO deposition was performed at 0.1 mbar by flowing 99.999% molecular oxygen into the chamber. The InP substrates, located at 6 cm from the target, were held at 623 K during deposition. The deposition conditions were chosen previously [11] in order to optimize the crystallinity of the ZnO films PLD-deposited on InP(100). The film thicknesses were measured with a Taylor–Hobson profilometer (Talysurf 50). ZnO films were deposited at a growth rate of 0.08 nm s^{-1} from very short deposition times (i.e. 180 s) up to relatively long times (i.e. 5 hours) in order to study the growth dynamics.

The film morphology was characterized by atomic force microscopy (AFM) by using a Nanoscope III equipment operating in tapping mode. Silicon cantilevers were employed (nominal radius of 10 nm). For each sample different images, with sizes from 0.2 μm up to 10 μm, were taken at different sample spots.

The parameters σ and ξ are obtained from the surface morphology $h(\boldsymbol{r}, t)$, measured by AFM. σ is defined as $\sigma = \langle [h(\boldsymbol{r}, t) - \langle h \rangle]^{1/2} \rangle$ where $\langle\rangle$ is the spatial average over the measured area. The value of σ is obtained directly from the AFM images taken on large surface areas by the AFM software. The lateral correlation length, ξ, is related to the lateral size of the surface features such as granular or pyramid structures for our system. The average value of ξ is obtained in this work from the crossovers of the power spectral density (PSD) of the AFM images [1, 2]. The PSD curves are provided by the AFM software. The so obtained ξ values agree with the average grain size measured directly on the corresponding AFM images. Also, the ξ values obtained for the pyramid structures are in agreement with those obtained from x-ray measurements using the Scherrer expression [12, 13].

Finally, the other important morphological parameter is the slope of the facets of the pyramid structures. This parameter is measured directly by the AFM software on those pyramids displaying a clear slope. The final slope value is obtained after averaging many individual measurements. This different procedure explains the relatively high error bars for these measurements.

3. Results and discussion

Figure 1 shows AFM images of the ZnO film surface for five different deposition times. The surface roughening is evident. For short deposition times, up to ≈ 2500 s, the surface

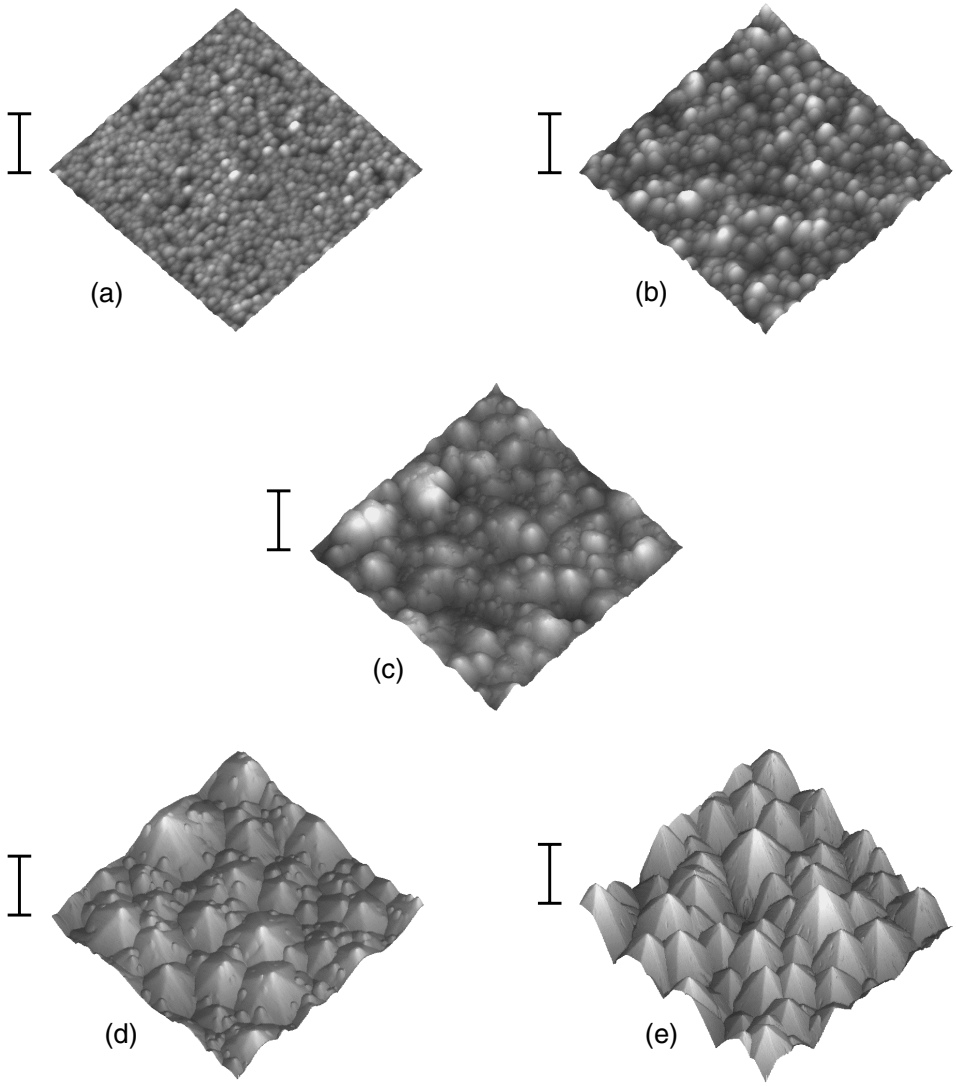

Figure 1. AFM images of a ZnO film grown after (a) 420 s, (b) 2100 s, (c) 2600 s, (d) 3000 s and (e) 18000 s. The scanned area is 1×1 μm^2 for deposition times shorter than 18000 s (a–d) and 3×3 μm^2 for 18000 s (e). The vertical bar indicates (a–d) 200 nm and (e) 300 nm.

morphology is mainly formed by a granular structure. After 2500 s of deposition a large coarsened structure appears underneath the granular structure. As the deposition time further increases the large structure, which grows both in width and height, tends to display a sixfold pyramid symmetry. The small granular structure, which is scattered on the large one, is still present although to a lesser extent. For long deposition times six-fold pyramid structures are clearly developed, growing in size with time, both laterally and vertically. The small granular structure completely disappears. It is worth mentioning that higher resolution AFM images taken on well developed pyramid facets reveal the existence of terraces and steps, which, after analysis of the step arrangement from AFM images, are not associated with the existence of dislocations. Figure 2 shows these steps after subtraction of the average facet plane. The steps

are $\approx$ 1 nm high, which corresponds to two ZnO lattice parameters along the [0001] direction. Thus, it is evident that two morphological growth behaviours are observed, separated by a crossover at $\approx$ 2500 s. The first one displays a granular structure and the second one a pyramid-like morphology.

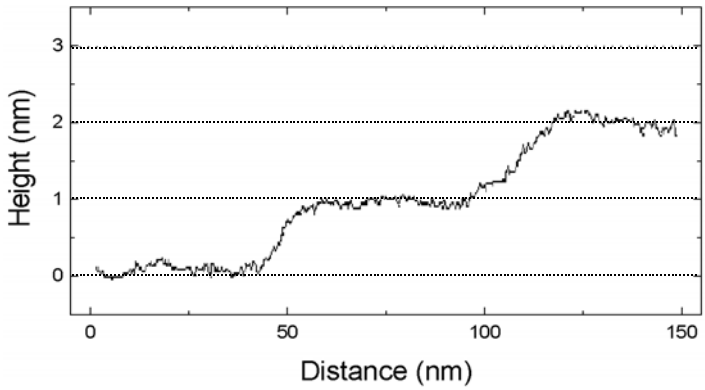

Figure 2. Surface profile taken from an AFM image of a pyramid face for the ZnO film deposited after 18000 s. The step height is $\approx$ 1 nm. It should be noted that the average slope of the pyramid face has been subtracted in order to clearly observe the surface steps. Otherwise, the 1 nm high steps would be masked by the steep morphology of the pyramid faces.

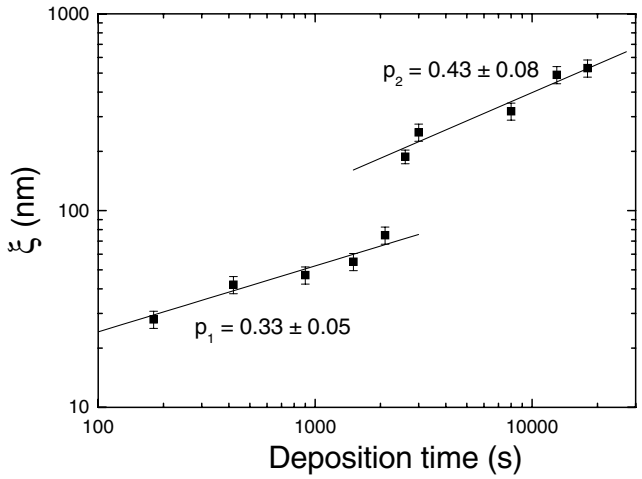

Figure 3. Logarithmic plot of the temporal evolution of the correlation length, ξ. Two regimes can be distinguished separated by a sharp crossover at $\approx$ 2500 s. The lines are the best fits obtained for both regimes.

Figure 3 shows the temporal evolution of ξ. Two temporal regions can be distinguished separated by a sharp crossover around 2000–3000 s. In the first region ranging up to $\approx$ 2500 s, a coarsening exponent of $p_1 = 0.33 \pm 0.05$ is found. In the second regime, for times longer than 2500 s, a coarsening exponent $p_2 = 0.43 \pm 0.08$ is observed. The sharp crossover between these two regions corresponds to the onset and fast formation of the pyramidal structure.

Figure 4 shows the change of the surface roughness, σ, with deposition time. A detailed analysis of figure 4 shows that two regions with a crossover at $\approx$ 2500 s are also observed

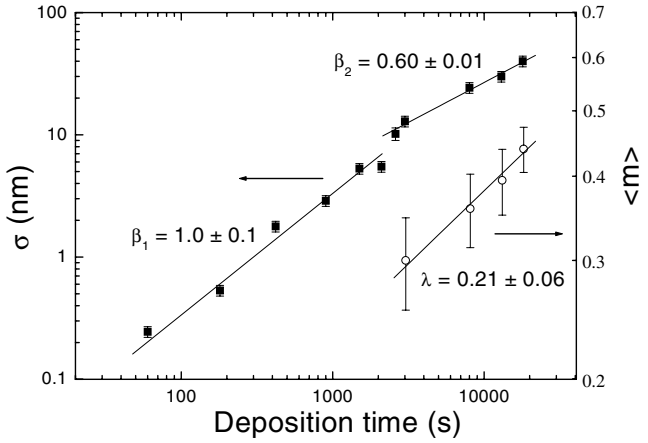

Figure 4. Left y-axis logarithmic plot of the temporal evolution of the surface roughness, σ (■). Two regimes can be distinguished separated by the same crossover than in figure 3. The lines are the best fits obtained for both regimes. Right y-axis logarithmic plot of the temporal evolution of the average pyramid slope, $\langle m \rangle$ (◯). The line represents the best fit obtained.

for the evolution of the surface roughness, although they are not so evident as in the case of figure 3. However, both the existence of two different morphology regions and two coarsening regimes with the same temporal crossover support the existence of these two regions also for the roughness evolution. Thus, the first region, for $t \leqslant 2000$ s, shows $\beta_1 = 1.0 \pm 0.1$ whereas for the second one, for $t \geqslant 3000$ s, $\beta_2 = 0.60 \pm 0.01$.

ZnO films do not display any order in the substrate plane as it is observed by x-ray pole figure [11]. However, θ-2θ x-ray diffraction spectra of the ZnO films only show from the early growth stages, besides of the peaks due to the InP (100) substrate, the peaks due to the $\langle 0001 \rangle$ ZnO planes. This fact is inconsistent with the Van der Drift model for polycrystalline growth [14, 15], in which a competitive growth between the different oriented crystals occurs.

From the evident improvement of the surface crystallinity with deposition time (i.e. the apparition and further development of the pyramid structures) it can be interesting to assess the film crystallinity for the different deposition times. This analysis is showed in figure 5(a) where the film crystallinity figure of merit (see figure 5 caption for definition) is plotted versus deposition time. It is observed that the film crystallinity continuously improves until 3000 s and it saturates for times longer than 5000 s.

In summary, the experimental results indicate that the growth dynamics of ZnO films grown by PLD on InP(100) substrates presents two growth regimes. The first one, for $t \leqslant 2500$ s, is characterized by the exponents $p_1 = 0.33$ and $\beta_1 = 1$; whereas the second one, for $t \geqslant 3000$ s, has $p_2 = 0.43$ and $\beta_2 = 0.60$. Both regions present growth exponents that are characteristics of unstable growth processes (i.e. $\beta \geqslant 0.5$) [1]. The first zone is characterized by the existence of a granular structure without any preferred surface orientation whereas the second one is characterized by the development, both in lateral size and height, of a pyramidal structure whose facets exhibit a stepped morphology. For this second regime the corresponding film cristallinity attains the saturation value, which is much higher than that observed for the first growth regime.

The first regime presents a coarsening exponent consistent with that one predicted by the shadowing models for 2+1 dimensions [16]. The high β_1 value also agrees with this interpretation [16] as it corresponds to the surface roughening process induced by the

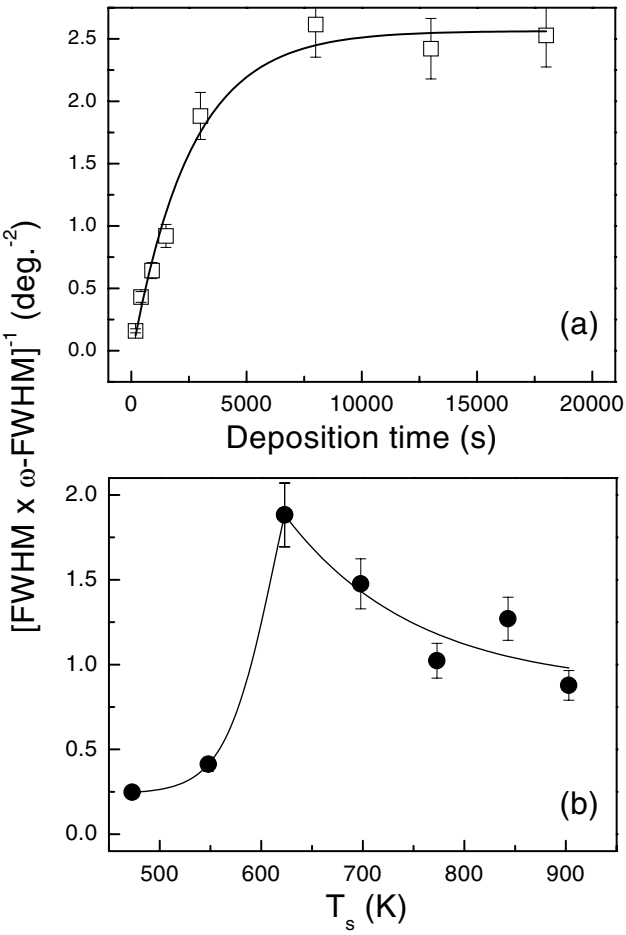

Figure 5. Cristallinity figure of merit (θ-FWHMx ω-FWHM)$^{-1}$ of ZnO deposited as a function of a) the deposition time and b) the substrate temperature (T_s). θ-FWHM and ω-FWHM correspond to the full width at half maximum of the X-ray diffraction measured in $\theta - 2\theta$ and ω scan (i.e. rocking curve around to 002 ZnO diffractions), respectively [11].

competitive growth of the different surface structures.

During PLD a high-density sharp plume of ablated species is produced. In the presence of a background gas, the plume angular distribution is broadened due to the scattering of the ablated species with the background gas molecules. This broadening effect is more important for slighter species. Under our experimental conditions ($p_{oxygen} = 0.1$ mbar) we have checked that the plume angular aperture angle is as large as 34°. Therefore, the arriving materials do not impinge normally on the growing surface but rather with a given incident angular distribution. Thus, the most prominent surface structures will shadow those located at more depressed surface regions and will show a higher growth rate characteristic of competitive growth processes.

Finally, it is worth mentioning that we have performed the collapse of the PSD curves for the different deposition times following previous works on shadowing models [16]. The results obtained, which are shown in figure 6, display a good data collapsing following the scaling behaviour for the roughening and coarsening processes predicted by the shadowing

models. This collapse is observed for length scales smaller than the corresponding coarsening length (i.e. grain size). However, it is important to note that this data collapsing was only obtained for the first growth regime ($t < 3000$ s). This result also supports the existence of two different growth regimes both for the coarsening and roughening processes.

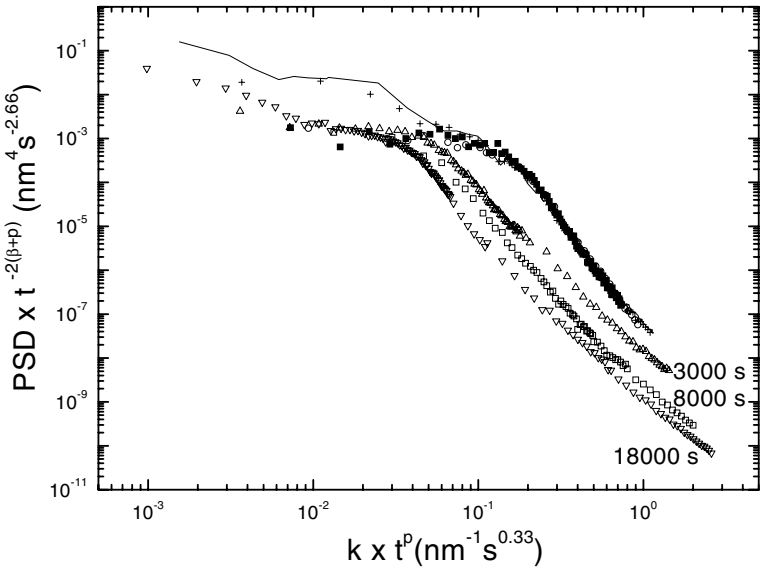

Figure 6. Scaling plots of the PSD curves for different deposition times: 420 s (■), 900 s (◯), 1500 s (+), 2100 s (solid line), 3000 s (△), 8000 s (□) and 18000 s (▽). The scaling plots are obtained by plotting $t^{2(p+\beta)}\ x\ PSD(k)$ versus $t^p x\ k$ [16], where $p = 0.33$ and $\beta = 1$. Note, that the collapse is verfied only for those films grown for times shorter than 3000 s.

The second regime corresponds also to unstable growth ($\beta_2 > 0.5$) and it is characterized by the development of a pyramidal structure with stepped surfaces. At this point it is interesting to note that the (0001) surface of PLD deposited ZnO, which is accepted to be usually O-terminated and quite polar [17], presents a relatively high density of step edges [18]. At step edges there is a higher electronic density than on the terraces because of the lower atom coordination and the localized nature of the dangling bonds. This situation would lead to the existence of electronic barriers at the steps for an atom diffusing on a terrace. Thus, the (0001) ZnO surface results to be prone to present step-edge barriers. The existence of steps has been shown in figure 2 together with the evident apparition and further development of pyramids. Step-edge barrier effects are unlikely in polycrystalline systems with randomly small grains [5]. This is not the case for our system since the pyramids are wider than 0.5 μm for the 1.5 μm thick film. Thus, the physical properties of our system and the morphological observations are consistent, in principle, with a pyramidal growth process influenced by the presence of step-edge barrier effects.

Most theoretical and experimental works considering the role of step-edge effects are related to single crystal and homoepitaxial growth systems [19, 20], particularly to metallic systems. Recently, step-edge effects have been invoked to partially explain the surface roughening of sputter-deposited polycrystalline nickel films [21]. In contrast, the importance of step-edge barriers in semiconductor materials is a much more debated question. Despite this ambiguity, this effect has been claimed to explain the roughening of systems such as Si(100) [22], Ge(001) [23] and GaAs(001) [24].

Although the β_2 value obtained is relatively high, β values equal or higher than 0.5 are predicted by different models considering step-edge effects [3, 19, 20, 25–27] depending on experimental conditions such as the magnitude of the step-barrier, deposition temperature, nearest-neighbour bonding magnitude and the possibility of post-deposition incorporation or relaxation. Besides, high experimental β values have been already explained under the frame of a growth behaviour induced by step-edge barriers. In particular, for Cu(100) a value of $\beta = 0.56$ has been reported [28] to be due to these effects. Also, for homoepitaxial growth of Ge(001) [29], although the film roughness does not follow a single power-law behaviour over the whole range of film thickness studied, a regime with $\beta \approx 0.5$ can be observed for the longest deposition times. Moreover, the value obtained for the coarsening exponent for this second regime, $p_2 = 0.43$, also agrees with predicted [28] and experimental [22] values for systems in which step barriers operate.

Thus, for the second growth regime observed in our system the roughening process proceeds at a higher rate than the coarsening one. At this point, it is useful to analyse the temporal evolution of the average pyramid slope, $\langle m \rangle$. This slope can remain constant or it can increase with time as $\langle m \rangle \sim t^{\lambda}$ [3]. The slope behaviour study is important since theoretical simulations [3] show that β values are in the 0.25-0.3 range if the slope stays constant whereas if $\langle m \rangle$ increases appreciably higher β values are observed. For pyramidal growth it is expected the following relationship $\beta = p + \lambda$ [3].

Figure 4 also shows the temporal evolution of $\langle m \rangle$, measured over the pyramidal surface features. The average slope increases from a value close to 0.3 after 3000 s to reach a value close to 0.44, with $\lambda = 0.21 \pm 0.06$. This value implies that the exponent relation $\beta = p + \lambda$ is obeyed in our case within the experimental errors. This slope increase is consistent with the high value of β_2 measured in the second growth regime. The higher error bar for the slope values for those films deposited for shorter times can be due to the fact that the pyramid structure at this growth stage is just emerging and coexisting with the granular structure, whereas at longer deposition times it is well defined.

From these results it can be concluded that the growth dynamic behaviour observed when the pyramid-like structures develop is consistent with that expected when step-barrier effects determine the growth mode. This behaviour is consistent with the observed sharp improvement of the film crystallinity for the second growth regime (figure 5(a)). This film crystallinity improvement, which is clearly associated with the formation and further development of the pyramid structures on the film surface, would lead to a better definition of step edges and terraces. This scenario is more favourable for the apparition of step-edge barrier effects. It must be noted that these effects should dominate over shadowing effects, which do operate during the whole growth process, after 2500 s of growth as they determine the observed growth behaviour.

A very useful parameter to assess the influence of step-edge barrier effects on the growth behaviour is the deposition temperature. However, this analysis is not suitable for our system since the film crystallinity, and therefore presumably the step-edge effects, changes sharply with the deposition temperature [11]. This is clearly observed in figure 5(b), which shows the plot of the film crystallinity figure of merit versus the deposition temperature. It is evident that the film crystallinity worsens for both higher and lower temperatures than that used in this work.

Whereas the simultaneous coarsening, stepping and roughening of the film surface are consistent with the theoretical [3, 19] and experimental [23] observations, the coarsening exponent value could be, to some extent, relatively high when it is compared to the theoretical predictions and most of the experimental values. This minor discrepancy can be due to different causes. First, it is known that the system symmetry can affect the coarsening exponent since

it has been reported [30, 31] that growth models with step-edge barrier effects and in-plane anisotropy lead to higher coarsening exponents than those without in-plane anisotropy. Second, it has been reported recently that a small amount of desorption dramatically speeds up the coarsening of a pyramid array leading to p values as high as 0.5 [32]. In fact, reevaporation of ZnO from the (0001) face of a single crystal has been reported for temperatures as low as 653 K, which is close to our deposition temperature [17, 33]. Third, it must be reminded that shadowing effects are present during the whole growth process. Thus, although these effects do not determine the growth behaviour they can still have influence on it in some extent. On the other hand, grain-boundary groove effects such as those reported for Al polycrystalline films [34] are not present since the coarsening process would lead to surface smoothing, because of the disappearance of grooves, rather than to surface roughening.

4. Conclusions

In conclusion, it has been observed that ZnO films grown by PLD on InP(100) substrates show a dynamic growth behaviour characterized by two different growth regimes separated by a sharp crossover. The first regime is dominated by shadowing effects due to the high-pressure deposition conditions that lead to the angular spreading of the incident depositing particles. The second regime is clearly associated both to the apparition and further development of a pyramidal structure on the film surface and to the clear improvement of the film crystallinity. The observed growth behaviour for this pyramidal structure is consistent with the existence of step-edge barrier effects, which is expected from the electronic properties of the ZnO surface. The competitive character of the coarsening and roughening processes, accompanied by the steeping process, originated by these effects is observed. Thus, for this second growth regime and under our experimental conditions, step-edge barrier effects are stronger than shadowing effects, determining the growth behaviour.

Ackowledgments

E Vasco is supported by a MUTIS grant. This work was sponsored by CAM 07T/0032/1997 project. We acknowledge fruitful discussions with Dr J A Martín-Gago and Dr R Cuerno.

References

[1] Barabási A L and Stanley H E 1995 *Fractal Concepts in Surface Growth* (Cambridge: Cambridge University Press)
[2] Meakin P 1998 *Fractals, Scaling and Growth Far from Equilibrium* (Cambridge: Cambridge University Press)
[3] Smilauer P and Vvedensky D 1995 *Phys. Rev.* B **52** 14263
[4] Palasantzas G and Krim J 1994 *Phys. Rev. Lett.* **73** 3564
[5] Jeffries J H, Zuo J K and Craig M M 1996 *Phys. Rev. Lett.* **76** 4931
[6] Schilardi P L, Azzaroni O, Salvarezza R C and Arvia A J 1999 *Phys. Rev.* B **59** 4638
[7] Combe N and Jensen P 1998 *Phys. Rev.* B **57** 15553
[8] Chrisey D B and Hubler G K (ed) 1994 *Pulsed Laser Deposition of Thin Films* (New York: Wiley) ch 14–16, 20 and 21
[9] Vispute R D, Talyansky V, Trajanovic Z, Choopun S, Downes M, Sharma R P, Woods M C, Lareau R T, Jones K A and Iliadis A A 1997 *Appl. Phys. Lett.* **70** 2735
[10] Tang Z K, Wong G K L, Yu P, Kawasaki M, Ohtomo A, Koinuma H and Segawa Y 1998 *Appl. Phys. Lett.* **72** 3270
[11] Vasco E, Rubio-Zuazo J, Vázquez L, Prieto C and Zaldo C 2001 *J. Vac. Sci. and Technol B* **19** 224
[12] Scherrer P 1918 *Göt. Nachr.* **2** 98
[13] Stokes A R and Wilson A J C 1942 *Proc. Camb. Phil. Soc.* **38** 313

[14] Van der Drift A 1967 *Philips Res. Rep.* **22** 267
[15] Thijssen J M 1995 *Phys. Rev.* B **51** 1985
[16] Yao J H and Guo H 1993 *Phys. Rev.* E **47** 1007
[17] Ohnishi T, Ohtomo A, Kawasaki M, Takahashi K, Yoshimoto M and Koinuma H 1999 *Appl. Phys. Lett.* **72** 824
[18] Parker T M, Condon N G, Linsay R, Leibsle F M and Thornton G 1998 *Surf. Sci.* **415** L1046
[19] Krug J 1997 *Adv. Phys.* **46** 139
[20] Politi P, Grenet G, Marty A, Ponchet A and Villain J 2000 *Physics Reports* **324** 271
[21] Saitou M, Makabe A and Tomoyose T 2000 *Europhys. Lett.* **52** 185
[22] Eaglesham D J and Gilmer G H 1992 *Surface disordering growth, roughening and phase transitions* ed R Jullien, J Kertész, P Meakin and D E Wolf (New York: Nova Science) p 69
[23] Van Nostrand J E, Chey S J, Hasan M A, Cahill D G and Greene J E 1995 *Phys. Rev. Lett.* **74** 1127
[24] Orme C, Johnson M D, Sudijono J L, Sander L M and Orr B G 1994 *Phys. Rev. Lett.* **72** 116
[25] Siegert M and Plischke M 1994 *Phys. Rev.* E **50** 917
[26] Golubovic L 1998 *Phys. Rev. Lett.* **78** 90
[27] Biehl M, Kinzel W and Schinzer S 1998 *Europhys. Lett.* **41** 443
[28] Ernst H J, Fabre F, Folkerts R and Lapujoulade J 1994 *Phys. Rev. Lett.* **72** 112
[29] Van Nostrand J E, Chey S J and Cahill D G 1995 *J. Vac. Sci. Technol.* B **13** 1816
[30] Siegert M 1998 *Phys. Rev. Lett.* **81** 5841
[31] Amar J G 1999 *Phys. Rev.* B **60** 11317
[32] Smilauer P, Rost M and Krug J 1999 *Phys. Rev.* E **59** R6263
[33] Kohl D, Henzler M and Heiland G 1974 *Surf. Sci.* **41** 403
[34] Lita A E and Sanchez J E Jr 2000 *Phys. Rev.* B **61** 7692